ChemComm

COMMUNICATION

View Article Online
View Journal | View Issue

Cite this: *Chem. Commun.*, 2016, 52, 2784

Received 15th September 2015,
Accepted 4th January 2016

DOI: 10.1039/c5cc07726e

www.rsc.org/chemcomm

DNA aptamer release from the DNA–SWNT hybrid by protein recognition†

Chang-Hyuk Yoo,[ab] Seungwon Jung,[abc] Jaehyun Bae,[d] Gunn Kim,[e] Jisoon Ihm[d] and Junghoon Lee*[ab]

Here we show the formation of the complex between a DNA aptamer and a single-walled carbon nanotube (SWNT) and its reaction with its target protein. The aptamer, which is specifically bound with thrombin, the target protein in this study, easily wraps and disperses the SWNT by noncovalent π–π stacking.

Aptamers are oligonucleotides which can recognize various targets such as small molecules, proteins, and cells as well as inhibit the function of the biomolecules.[1–5] The aptamers are regarded as an ideal alternative to the antibodies for biomolecular applications such as screening, diagnostics, and therapy due to their high affinity, selectivity, and stability.[6–9] They identify target molecules through conformational recognition which is achieved by inter- or intra-hydrogen bonding in nucleic acids.[10] One of the unique properties of the DNA aptamers as compared with antibodies is the degree of freedom of its conformations. The DNA aptamers can exist in the form of single-stranded DNA (ssDNA), which can be freely suspended in the solution, or double-stranded DNA (dsDNA), which is produced by the reaction with its complementary DNA, complex with the target molecule, and complex with other platforms to generate the signal or be delivered to a specific target.[11–13] To predict and understand the forms of the aptamer under given conditions and its transformation to others are important to use the aptamer suitably, especially when using in a complex form with other molecules.

The combination with nanomaterials has been studied for increasing the flexibility of the aptamers in recent years. Various nanomaterials such as gold nanoparticles, quantum dots, liposomes, and other nanoelements have been used as associating agents.[14–17] Single-walled carbon nanotubes (SWNTs) have also caught attention for combining with the aptamers due to their unique mechanical, electrical, and chemical properties.[18–20] Since DNA can disperse the SWNTs through noncovalent π–π stacking, DNA aptamers can be linked to the SWNTs without covalent bonding.[21–25] Our group previously showed a hybrid formation between ssDNA and the SWNTs using the aforementioned noncovalent π–π stacking.[26] In addition, we verified the dissociation of the DNA from the SWNT because of the interaction with its complementary DNA.[27] Hydrogen bonding between the DNAs is stronger than the π–π stacking between the DNA and the SWNT. Thus DNA should be detached as it meets and reacts with its complementary DNA. Our interest has moved to the interaction of the DNA aptamer in the aptamer–SWNT hybrid with its target protein.

Here we demonstrate the formation of aptamer–SWNT hybrids and the detachment of the aptamer from the SWNT due to the reaction with its target protein. The thrombin binding aptamer is selected as a wrapping agent for the SWNT, and thrombin is used as a target in this work. The changes in the electronic structure of the SWNTs by wrapping and unwrapping processes were observed by Raman spectroscopy, and the conformational change of the aptamer upon combining with the SWNT and reacting with its target protein was measured by circular dichroism spectroscopy. The experiments confirm that the aptamer helically wraps the SWNT like dsDNA and this aptamer is released from the SWNT upon reacting with the target protein. Molecular dynamics (MD) simulations for binding free energy were performed to theoretically study the conformational change and its mechanism in detail.

The aptamer–SWNT hybrids have been produced through the sonication and centrifugation with the thrombin binding aptamer in D.I. water. The reaction of the aptamer–SWNT hybrid with the protein was carried out by adding thrombin as a target, and bovine serum albumin (BSA) as a negative control into aptamer–SWNT hybrid solution, respectively. Then the mixtures of the hybrids and the proteins were kept at room

[a] *School of Mechanical and Aerospace Engineering, Seoul National University, Seoul 151-742, Republic of Korea. E-mail: jleenano@snu.ac.kr*
[b] *Inter-Semiconductor Research Center, Seoul National University, Seoul 151-742, Republic of Korea*
[c] *Center for Biomicrosystems, Korea Institute of Science and Technology, Seoul 136-791, Republic of Korea*
[d] *FPRD and Department of Physics and Astronomy, Seoul National University, Seoul 151-742, Republic of Korea*
[e] *Department of Physics, Sejong University, Seoul 143-747, Republic of Korea*
† Electronic supplementary information (ESI) available. See DOI: 10.1039/c5cc07726e

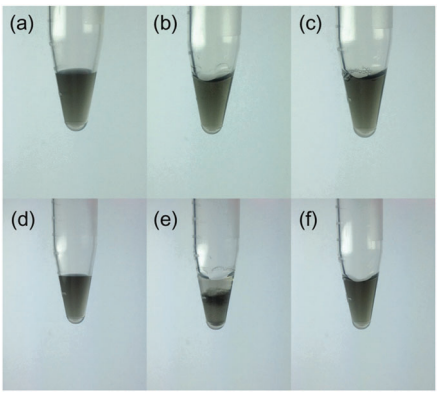

Fig. 1 The photographs of the aptamer–SWNT hybrid before and after the reaction with the protein, (a) and (d): the hybrid itself, (b) and (e): the mixture 1 between the hybrid and thrombin, (c) and (f): the mixture 2 between the hybrid and BSA. The uppers were taken right after the reaction and the lowers were done 1 h later. After 1 h, only mixture 1 showed precipitation at the bottom.

temperature without any further treatment. The SWNTs in the sample in which thrombin was introduced began to aggregate and form a precipitate at the bottom of the solution and they were fully deposited at the bottom after 1 h (in Fig. 1), which is caused by the detachment of the aptamers from the SWNTs due to affinity difference. While the aptamer–SWNT hybrid is formed only by π–π stacking between the bases of the DNA and the hexagonal ring structure in the SWNTs, the aptamer–target protein binding structure is formed by stacking interactions, shape complementarity, electrostatic interactions, and hydrogen bonding.[28] Therefore, the binding of the aptamer with the target protein instead of the SWNT is more favourable. In contrast to the reacted sample with thrombin, the aptamer–SWNT hybrids with BSA or nothing were not aggregated or precipitated. This means that no reaction occurred in these solutions because the hybrids were stable in DI water and the affinity with non-target proteins was not high enough to detach the wrapping aptamer from the SWNT. The UV/vis/NIR spectra of the samples clearly showed relatively quantitative results regarding the amount of remaining hybrids after the reaction (ESI,† S3). After BSA injection, the intensity of the spectrum showed no difference according to the concentration of the BSA. However, the intensity after thrombin injection became lower upon increasing the concentration of the thrombin. Based on these observations, we concluded that unwrapping of the aptamer by recognition of the protein was a target-specific event.

To investigate the detachment of the aptamer from the SWNT, the Raman spectra of the samples were observed, which is useful for studying unwrapping of the DNA from the SWNT by measuring the change in the Breit–Wigner–Fano (BWF) line shape.[26] The majority of the diameters of the SWNTs were estimated to about 1.1 nm for every sample through analysis of the peak at radial breathing modes (RBMs, 270 cm^{-1})[29] (ESI,† S5). To see the change in the BWF line shape according to the reaction with the protein, every measurement was carried out at pH 3. This acidic condition was a key factor in this study because the basic environment of the solution induced by the protein distorted the BWF line shape of the SWNT (ESI,† S4). After wrapping of the aptamer around the SWNT, the BWF line shape was shifted to a higher frequency and its magnitude was diminished, which indicates that the electronic structure of the SWNT was changed by wrapping of the aptamer. This transition of the BWF line shape by wrapped DNA around the SWNT was previously explored.[26]

This transition has returned back by the injection of the thrombin into the hybrid solution. The SWNT after the reaction with thrombin showed a strong BWF line shape again unlike the hybrid before the reaction. It means that the reaction with the target protein leads to the release of the aptamer from the SWNT and then the electronic properties of the SWNT return back to the original state representing the strong BWF line shape. This phenomenon looks very similar to the previous results achieved with its complementary DNA.[27] In contrast, the hybrid with BSA showed no significant difference in the BWF line shape from the hybrid (Fig. 2). This is clear evidence for the specific reactivity of the hybrid.

The structure of the DNA aptamer when wrapping the SWNT or upon detachment from the SWNT is important for the estimation of the aptamer/SWNT hybrid structure. In the case of the thrombin binding aptamer we used in this study, two main peaks are shown in the CD spectrum when it forms the G-quartet structure; one is negative at around 270 nm and another is positive at around 295 nm.[30] The intensity of the spectrum represents the amount of G-quartet structures in the analyte. Fig. S1 (ESI,†) shows the CD spectra of aptamer, thrombin, aptamer–SWNT hybrids, SWNT after reaction with thrombin, and the hybrids reacted with thrombin (ESI,† S2). When the aptamer was dissolved in D.I. water, its spectrum clearly represented the formation of the G-quartet structure which is a secondary structure of the thrombin binding aptamer. In contrast, when the aptamer wrapped around the SWNT, the resulting hybrid showed a different shape from the initial CD spectrum of the only aptamer, which has reverse peaks: positive at around 270 nm and negative at around 295 nm. This spectrum is similar to the general spectrum of b-type double stranded DNA, which indicates the helical wrapping of the aptamer around the SWNT similar to double stranded DNA.[31] The CD spectra showed the structural change of the aptamer by the reaction with thrombin.

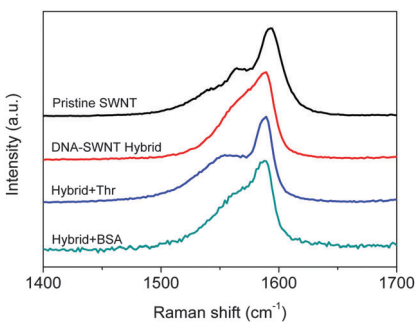

Fig. 2 G-modes of the four samples; pristine SWNT, hybrid, the mixture 1 between the hybrid and thrombin, and mixture 2 between the hybrid and BSA. The Breit–Wigner–Fano line shape which was shown in pristine SWNTs disappeared after hybrid formation with the aptamer, and then it returned back to initial line shape due to the reaction with thrombin.

Table 1 Relative binding free energy of the aptamer DNA–thrombin hybrid and the aptamer DNA–SWNT hybrid. The energy unit is kcal mol^{-1}

Configurations	Aptamer–thrombin complex and separated SWNT [Fig. 3(a)]	Aptamer–thrombin hybrid and separated thrombin [Fig. 3(b)]	SWNT, aptamer and thrombin. All molecules are separated. (reference)
Interaction energy	−221.5	−125	0
TS	−51.9	−41	0
Free energy	−169.6	−84	0

To see the pure spectrum of the solution, in which the strong thrombin peak was excluded, the spectrum of the solution after the reaction with thrombin was obtained by the subtraction of the thrombin spectrum from that obtained after the reaction between the hybrid and thrombin. The CD spectrum of estimated DNA that revealed a negative peak around 260 nm and a positive peak at 290 nm after the reaction showed peaks for G-quartet structures. It means that the DNA aptamer was released from the SWNT by the reaction with thrombin and formed the G-quartet structure upon reacting with thrombin and some aptamer still remained on the SWNT even after the reaction. The unwrapping efficiency seemed to be half but we believe that it can be improved by external energy to increase the possibility for the hybrid and thrombin to react together in the solution. From CD spectroscopic analyses, it was confirmed that the structure of the aptamer with the SWNT is "helical wrapping" and this has been changed by the detachment of the aptamer from the SWNT upon reacting with thrombin.

Next, we performed molecular dynamics (MD) simulations using the Large-scale Atomic/Molecular Massively Parallel Simulator (LAMMPS) program to understand the atomistic mechanism of the formation of the DNA aptamer–SWNT hybrid and the reaction with its target protein observed in our experiment. The computational cost prohibited us from simulating the full time atomic dynamics in which the DNA aptamer is detached from the SWNT due to the binding with the target protein. Therefore, we just calculated the total free energies of various equilibrium atomic configurations and compared them. In each simulation, the binding free energies of biomolecular complexes were obtained by calculating the time-averaged free energy at equilibrium. Binding free energies consisted of the molecular energies of biomolecular complexes and the water-biomolecule interaction energy and the entropic contribution. For every 1 ps, the total energy was calculated and the 20 ns time average was used for analysis. The equilibrated atomic configuration was used to compute the entropic contribution to the binding free energy. The vibrational, translational, and rotational entropies were given by the following formulae:

$$-\mathrm{TS}_{\mathrm{vibration}} = -Tk_{\mathrm{B}} \sum_{\omega_i} \left[\frac{\beta h\omega_i}{\mathrm{e}^{\beta h\omega_i} - 1} - \log\left(1 - \mathrm{e}^{-\beta h\omega_i}\right) \right]$$

$$-\mathrm{TS}_{\mathrm{translation}} = -Tk_{\mathrm{B}} \left[\frac{5}{2} + \frac{3}{2}\log\left(\frac{2\pi m}{\beta h^2}\right) - \log\rho \right]$$

$$-\mathrm{TS}_{\mathrm{rotation}} = -Tk_{\mathrm{B}} \left[\frac{3}{2} + \frac{1}{2}\log(I_{\mathrm{a}} I_{\mathrm{b}} I_{\mathrm{c}}) + \frac{3}{2}\log\left(\frac{8\pi^2}{\beta h^2}\right) - \log\sigma \right]$$

where m is the mass of the molecule, $\beta = 1/k_{\mathrm{B}}T$ is the inverse temperature, h is the Planck constant, ρ is the number density, $I_{\mathrm{a/b/c}}$ is the moment of inertia, σ is the symmetry factor of the molecule, and ω_i is ith vibrational eigenfrequency of the molecule.[27] In this calculation, we set the number density and symmetry factor as 1 M L^{-1} and unity, respectively. These values are different from those of real materials, but the correction is very small because entropy depends logarithmically on them. Since the molecule has a large size ($\sim$5000 atoms in thrombin), and it is very difficult to calculate exact vibrational eigenfrequencies, we roughly estimated the vibrational entropy as described in the previous work.[27]

Table 1 summarizes the total binding free energies of the aptamer–SWNT hybrid (aptamer DNA wrapped around the SWNTs) and the aptamer–thrombin complex. In these MD simulations, the atomic coordinates of the aptamer–SWNT hybrid and the aptamer–thrombin complex were taken from previous MD simulations by Johnson *et al.* and by Jayapal *et al.* respectively.[32,33] The total binding free energy of the aptamer-thrombin complex is larger by 85.6 kcal mol^{-1} than that of the aptamer–SWNT hybrid. This affinity difference induces the aptamer to become detached from the SWNT and to bind with the thrombin. To verify that the SWNT is completely detached from the aptamer–thrombin complex, we compared the binding free energies of possible SWNT–aptamer–thrombin three molecular complexes shown in Fig. 4. The SWNT was completely detached and separated from the aptamer–thrombin complex. These computational results are in good agreement with our experimental findings. The detailed values are summarized in Table 2.

In summary, we demonstrated the structure of the aptamer when interacting with the SWNT and the detachment of the aptamer from the SWNT through the reaction with the target protein using the optical measurement techniques such as Raman and CD spectroscopy. In the Raman spectra, while the pristine SWNTs showed a strong BWF line shape, the SWNTs after the aptamer wrapping showed the attenuated BWF line shape due to the interaction between the SWNT and the aptamer. Upon the reaction with thrombin its optical properties returned to the initial state through the unwrapping process of the

Table 2 Relative free energy of aptamer–thrombin–SWNT (complex type 1). The energy is in unit of kcal mol^{-1}

	Aptamer–thrombin complex and SWNT	Aptamer–thrombin–SWNT complex
Free energy	Fig. 4(a) −1527 Fig. 4(c) −1739	Fig. 4(b) 0 Fig. 4(d) 0

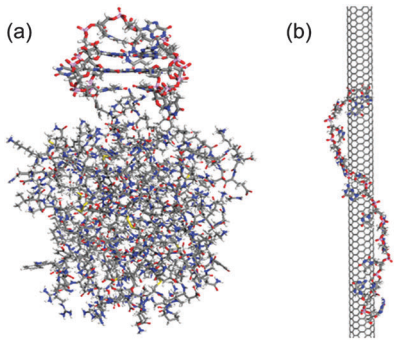

Fig. 3 (a) Simulation snapshot of the aptamer–thrombin complex. (b) Simulation snapshot of the aptamer–SWNT hybrid. Water molecules are omitted for visual clarity.

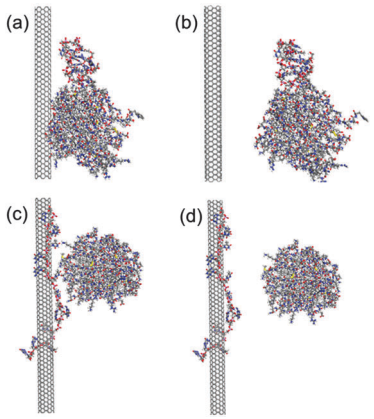

Fig. 4 Simulation snapshots of DNA aptamer, thrombin, and SWNT complexes. (a) Aptamer–thrombin complex near the SWNT. (b) Aptamer–thrombin complex separated from the SWNT. (c) Thrombin near the aptamer–SWNT hybrid. (d) Thrombin separated from the aptamer–SWNT hybrid. Water molecules are omitted for visual clarity.

aptamer from the SWNT. The CD spectrum of the aptamer after wrapping the SWNT showed no G-quartet structure but the peaks similar to double stranded DNA due to helical wrapping around the SWNT. On the other hand, it showed the peaks representing the G-quartet structure after the specific reaction with thrombin. The MD simulations and binding energy calculations provided an atomistic description of the pathway to this phenomenon. Based on the calculations, we verified that the reaction of the aptamer with thrombin is more favourable than that with the SWNT and the aptamer–thrombin complex is completely detached from the SWNT. We believe that this observation will improve the understanding of the structure of nanomaterial–biomolecule conjugates and open up a new approach for biological applications such as apta-sensors for various molecules.

This research was supported by the Center for Integrated Smart Sensors funded by the Ministry of Science, ICT & Future Planning as Global Frontier Project (CISS-2011-0031866), and by BioNano Health-Guard Research Center funded by the Ministry of Science, ICT & Future Planning (MSIP) of Korea as Global Frontier Project (Grant number H-GUARD_2015M3A6B2068409).

Notes and references

1 A. D. Ellington and J. W. Szostak, *Nature*, 1990, **346**, 818–822.
2 M. Famulok, *Curr. Opin. Struct. Biol.*, 1999, **9**, 324–329.
3 S. Weiss, D. Proske, M. Neumann, M. H. Groschup, H. A. Kretzschmar, M. Famulok and E. L. Winnacker, *J. Virol.*, 1997, **71**, 8790–8797.
4 J. K. Herr, J. E. Smith, C. D. Medley, D. H. Shangguan and W. H. Tan, *Anal. Chem.*, 2006, **78**, 2918–2924.
5 L. C. Bock, L. C. Griffin, J. A. Latham, E. H. Vermaas and J. J. Toole, *Nature*, 1992, **355**, 564–566.
6 D. H. J. Bunka, O. Platonova and P. G. Stockley, *Curr. Opin. Pharmacol.*, 2010, **10**, 557–562.
7 M. Cha, J. Shin, J. H. Kim, I. Kim, J. Choi, N. Lee, B. G. Kim and J. Lee, *Lab Chip*, 2008, **8**, 932–937.
8 E. J. Cho, J. W. Lee and A. D. Ellington, *Annu. Rev. Anal. Chem.*, 2009, **2**, 241–264.
9 W. H. Tan, H. Wang, Y. Chen, X. B. Zhang, H. Z. Zhu, C. Y. Yang, R. H. Yang and C. Liu, *Trends Biotechnol.*, 2011, **29**, 634–640.
10 T. Hermann and D. J. Patel, *Science*, 2000, **287**, 820–825.
11 O. C. Farokhzad, J. J. Cheng, B. A. Teply, I. Sherifi, S. Jon, P. W. Kantoff, J. P. Richie and R. Langer, *Proc. Natl. Acad. Sci. U. S. A.*, 2006, **103**, 6315–6320.
12 R. F. Macaya, P. Schultze, F. W. Smith, J. A. Roe and J. Feigon, *Proc. Natl. Acad. Sci. U. S. A.*, 1993, **90**, 3745–3749.
13 Y. Xiao, B. D. Piorek, K. W. Plaxco and A. J. Heeger, *J. Am. Chem. Soc.*, 2005, **127**, 17990–17991.
14 Z. H. Cao, R. Tong, A. Mishra, W. C. Xu, G. C. L. Wong, J. J. Cheng and Y. Lu, *Angew. Chem., Int. Ed.*, 2009, **48**, 6494–6498.
15 M. Ikanovic, W. E. Rudzinski, J. G. Bruno, A. Allman, M. P. Carrillo, S. Dwarakanath, S. Bhahdigadi, P. Rao, J. L. Kiel and C. J. Andrews, *J. Fluoresc.*, 2007, **17**, 193–199.
16 J. H. Lee, M. V. Yigit, D. Mazumdar and Y. Lu, *Adv. Drug Delivery Rev.*, 2010, **62**, 592–605.
17 J. Liu and Y. Lu, *Nat. Protoc.*, 2006, **1**, 246–252.
18 S. Frank, P. Poncharal, Z. L. Wang and W. A. de Heer, *Science*, 1998, **280**, 1744–1746.
19 A. Krishnan, E. Dujardin, T. W. Ebbesen, P. N. Yianilos and M. M. J. Treacy, *Phys. Rev. B: Condens. Matter Mater. Phys.*, 1998, **58**, 14013–14019.
20 J. Li, A. Cassell, L. Delzeit, J. Han and M. Meyyappan, *J. Phys. Chem. B*, 2002, **106**, 9299–9305.
21 H. Chen, C. Yu, C. M. Jiang, S. Zhang, B. H. Liu and J. L. Kong, *Chem. Commun.*, 2009, 5006–5008.
22 Y. C. Fu, T. Wang, L. J. Bu, Q. J. Xie, P. H. Li, J. H. Chen and S. Z. Yao, *Chem. Commun.*, 2011, **47**, 2637–2639.
23 S. M. Taghdisi, P. Lavaee, M. Ramezani and K. Abnous, *Eur. J. Pharm. Biopharm.*, 2011, **77**, 200–206.
24 Y. F. Zhang, B. X. Li, C. G. Van and L. H. Fu, *Biosens. Bioelectron.*, 2011, **26**, 3505–3510.
25 Z. Zhu, Z. W. Tang, J. A. Phillips, R. H. Yang, H. Wang and W. H. Tan, *J. Am. Chem. Soc.*, 2008, **130**, 10856.
26 M. Cha, S. Jung, M.-H. Cha, G. Kim, J. Ihm and J. Lee, *Nano Lett.*, 2009, **9**, 1345–1349.
27 S. Jung, M. Cha, J. Park, N. Jeong, G. Kim, C. Park, J. Ihm and J. Lee, *J. Am. Chem. Soc.*, 2010, **132**, 10964–10966.
28 S. B. Long, M. B. Long, R. R. White and B. A. Sullenger, *RNA*, 2008, **14**, 2504–2512.
29 R. Saito, T. Takeya, T. Kimura, G. Dresselhaus and M. S. Dresselhaus, *Phys. Rev. B: Condens. Matter Mater. Phys.*, 1998, **57**, 4145–4153.
30 S. Nagatoishi, Y. Tanaka and K. Tsumoto, *Biochem. Biophys. Res. Commun.*, 2007, **354**, 837–838.
31 J. Kypr, I. Kejnovska, D. Renciuk and M. Vorlickova, *Nucleic Acids Res.*, 2009, **37**, 1713–1725.
32 R. R. Johnson, A. C. Johnson and M. L. Klein, *Nano Lett.*, 2008, **8**, 69–75.
33 P. Jayapal, G. Mayer, A. Heckel and F. Wennmohs, *J. Struct. Biol.*, 2009, **166**, 241–250.